

Cosmogenic ^{10}Be dating of Guxiang and Baiyu Glaciations

ZHOU ShangZhe^{1†}, XU LiuBing¹, PATRICK M. Colgan², DAVID M. Mickelson³, WANG XiaoLi⁴, WANG Jie⁴ & ZHONG Wei¹

¹ Department of Geography, South China Normal University, Guangzhou 510631, China;

² Department of Geology, Grand Valley State University, Allendale, Michigan 49401, USA;

³ Department of Geology and Geophysics, University of Wisconsin-Madison, Madison, Wisconsin 53706, USA;

⁴ Department of Geography, Lanzhou University, Lanzhou 730000, China

Guxiang and Baiyu Glaciations are two previously recognized local glaciations of the Tibetan Plateau. They have been widely used as the reference standard for classifying Late Quaternary glaciations on the Tibetan Plateau and its surrounding mountains. However, the numerical chronologies of both glaciations have been lacking. In this study, cosmogenic ^{10}Be dating was undertaken to define the timing of these two glaciations. The surface boulders deposited by the glaciers of the Guxiang and Baiyu Glaciations have exposure ages of $112.9 \pm 16.7 - 136.5 \pm 15.8$ ka BP and $11.1 \pm 1.9 - 18.5 \pm 2.2$ ka BP, respectively. It is likely that the Guxiang and Baiyu Glaciations correspond to marine isotope stages 6 and 2, respectively.

Guxiang Glaciation, Baiyu Glaciation, cosmogenic ^{10}Be dating

The Guxiang and Baiyu Glaciations are two of the local glaciation events recognized on the Tibetan Plateau so far. These two glaciations were thought to be comparable with Riss and Würm Glaciations in the Alps, respectively^[1]. Subsequently, the two glaciations have been correlated with marine isotope stages 6 and 4 (MIS-6 and MIS-4)^[2]. In this study, we undertook terrestrial cosmogenic radionuclide surface exposure (SE) dating to define the timing of both glaciations.

1 Location and setting

The typical glacial landforms of the Guxiang and Baiyu Glaciations are present in the Bodui Zangbo River valley, adjacent to the Big Bend of the Yarlung Zangbo River in the southeastern part of the Tibetan Plateau (Figure 1). The Parlong Zangbo River, originating from the Laigu glacier, flows westward and joins the Yilong Zangbo River at Tongmai, and then flows 40 km southward eventually joining the Yarlung Zangbo River. The Yar-

lung Zangbo River turns 180° around the Namche Barwa Mountain, where the Big Bend forms, and then flows 200 km southward and eventually joins the Brahmaputra River in the Indian Plain. The Bodui Zangbo River, the largest tributary of the Parlong Zangbo River, originates from the glaciers of the eastern Nyainqêntanglha Mountains. Because abundant glacial sediments and well developed landforms are present in the Bodui Zangbo River valley we chose this area to date moraines.

When viewed at a large scale, the study area is located in the junction of the Himalayas, Nyainqêntanglha and Hengduan Mountains. Strong moisture from the Bengal Bay is delivered to this area by the south Asian monsoon through the Yarlung Zangbo River valley. The characteristics of this area can be described as follows: (1) An area with most precipitation on the Tibetan

Received August 8, 2006; accepted March 21, 2007

doi: 10.1007/s11434-007-0208-y

†Corresponding author (email: zhsz@lzu.edu.cn)

Supported by the National Natural Science Foundation of China (Grant Nos. 40371013 and 40601012) and NSF/EAR-0345277

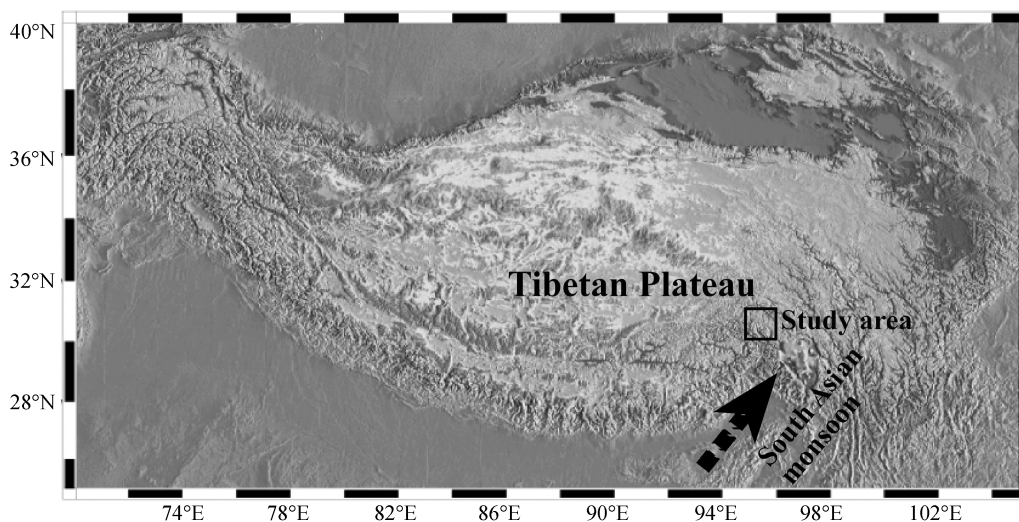


Figure 1 The study area on the Tibetan Plateau and the main path of the South Asian monsoon.

Plateau. The annual precipitation near the equilibrium line altitude (ELA) is ~ 3000 mm; (2) One of the areas having the lowest ELA. The contemporary ELAs in this area vary from 4500 m to 5000 m, equivalent to those in the Qilian Mountains 10 degrees latitude north of this area; (3) The most luxuriant original forest. There are abundant animal and plant species and complete altitudinal belts in this region. (4) The location of many of the contemporary maritime glaciers in China. Up to 28 glaciers over 10 km long are present in this area. The famous Qiaqing Glacier has a length up to 35 km and has an area of 151.5 km^2 ^[3]. The glaciers in this region are characterized by high temperature, high accumulation, fast flow, and intensive erosion ability. (5) An area where glacial extent changes most dramatically during the alternation of glacial and interglacial periods. Because there is abundant precipitation for glacier development, glaciers in this area are sensitive to temperature changes. Consequently, during the glacial periods with large depressions of temperature, such as the last glacial period, this area had the most extensive glaciation on the Tibetan Plateau^[4]. Today, when temperatures are higher the most extensive contemporary glaciers are in the Karakorum Mountains, Western Kunlun Mountains, and northwestern Tibetan Plateau.

Due to the high precipitation, intensive erosion and incision also occur in this area. Consequently, older glacial sediments are less well preserved than in dryer regions. The glacial sediments still preserved are typically younger than in other parts of the Plateau. During the comprehensive scientific investigation of Tibetan Pla-

teau in the 1970s, Li^[1] suggested two glaciation names, the Guxiang and Baiyu Glaciations, which subsequently became accepted as two representative local glaciation names. Guxiang and Baiyu Glaciations were considered to be equivalent to the Riss and Würm Glaciations in the Alps, corresponding to the Jilongsi and Rongbusi Glacial Stages in the Mt. Qomolangma area, respectively.

2 Glacial sediments and their distribution

There are 334 glaciers with a total area of 825.26 km^2 throughout the Bodui Zangbo drainage basin^[5]. At the headwaters of the Bodui Zangbo River is the Guanxing Glacier (Figure 2 (a)). The Zepu Glacier, having a length of 12 km and an area of 65.8 km^2 , is the longest one in this area. It terminates at an altitude of 3420 m above sea level (asl). The upper limit and the ELA of the Zepu Glacier have altitudes of 6349 m asl and 4683 m asl, respectively. Based on the glacial records, it can be inferred that all glaciers across the drainage basin flowed downward into the main valley and formed a huge complex valley glacier during glacial periods. A lateral moraine, preserved on the right side of the Bodui Zangbo River in Xumu, rises 500–800 m above the contemporary river valley and varies from 100 m to 200 m in width. The moraine first occurs at Yuren and extends southeastward along the right valley wall and eventually terminates at Badaka Village, where the Bodui Zangbo River joins Yalong Zangbo River. By contrast, the lateral moraine on the left side of the Bodui Zangbo River dis-

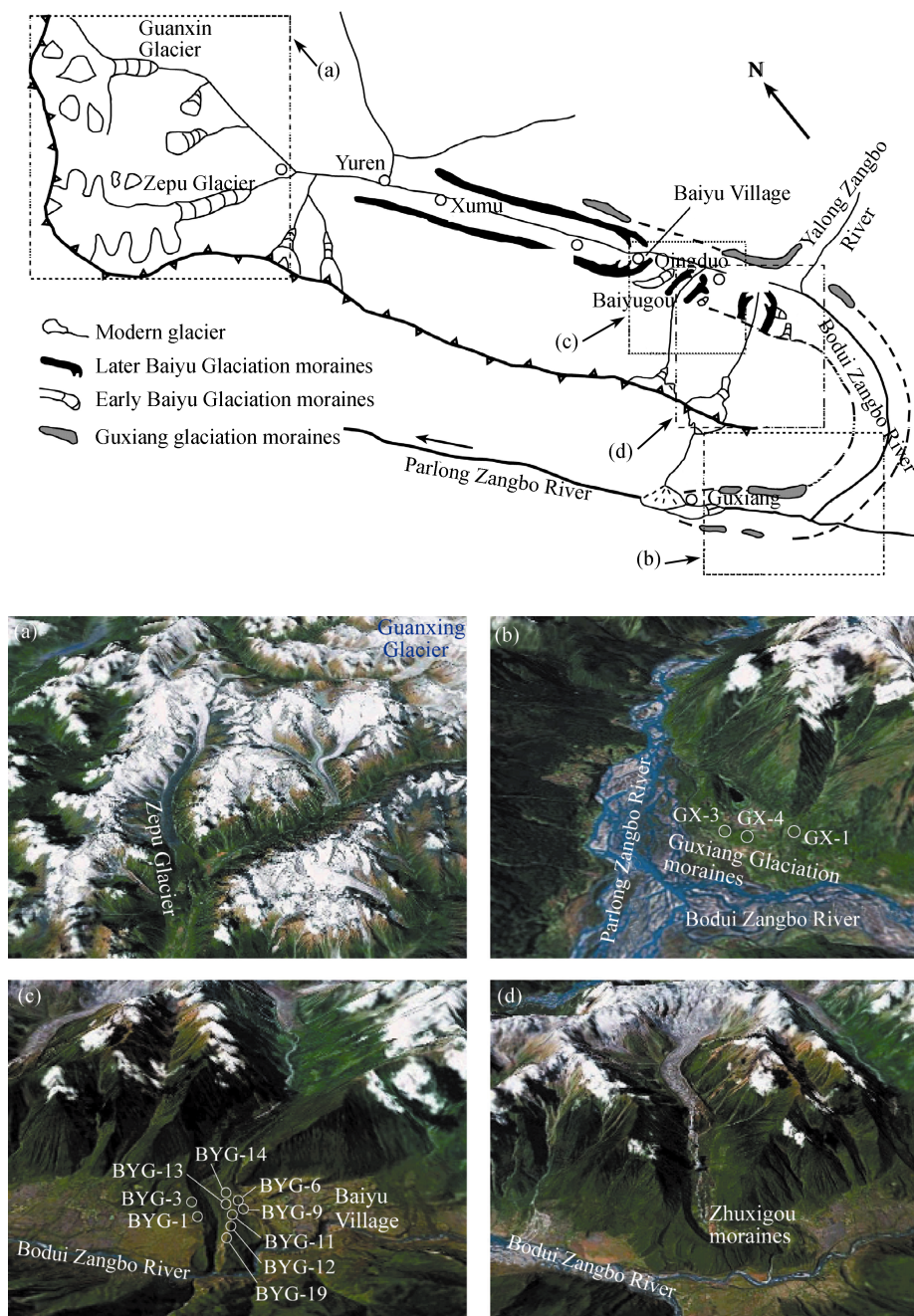


Figure 2 Outline of the Bodui Zangbo River valley showing the major moraines and the sample locations. (a) Zepu and Guanxing Glaciers; (b) sample locations of the Guxiang Glaciation moraines; (c) sample locations of the Baiyu Glaciation moraines; (d) Baiyu Glaciation moraines at the mouth of the Zhuxigou Valley.

continuously extends southeastward and terminates near Guxiang Village. A reconstruction based on this lateral moraine shows that the paleo-glacier had a length up to ~100 km. Consequently, the period during which this huge glacier advanced was named “Guxiang Glaciation”^[1]. At the Kada Bridge, where the Bodui Zangbo River joins the Palong Zangbo River, the lateral moraine rises 200–300 m above the contemporary river valley and has 2–3 km² of relative flat surface with 0.4 km² of

lake on it (Figure 2 (b)). Abundant granite boulders up to 3 m in diameter, exhibiting deep weathering on their surfaces, are present on the moraine crest outside the lake. Samples (GX-1, 3 and 4) were collected from these boulders (Figure 2(b)).

Baiyu Glaciation was suggested based on the moraines present in Baiyu (Figure 2(c)). A huge arc-shaped terminal moraine was deposited at Baiyu by the glaciers from the Bodui Zangbo River valley. It rises ~100 m

above the main river valley. Baiyu Village is located at the inner side of this moraine. Four sets of moraines, deposited by glacial advances from the Baiyugou Valley, are present outside the main valley moraine. The innermost set of moraines is larger than the outer three moraine sets, suggesting that the ice margin forming the innermost moraine set remained at its outermost position for a longer period than the other three glacial advances. Stratigraphically, the outer moraine sets are older than the inner ones. The moraine surfaces have abundant granitic boulders, from which samples (BYG-1, 3, 6, 9, 11, 12, 13, 14 and 19) were collected. The Zhuxigou Valley is located at the lower reach of the Bodui Zangbo River (Figure 2(d)). Moraine distribution in the Zhuxigou valley is similar to that in the Baiyugou Valley. The main valley glacier formed by the tributary glaciers such as Guanxing and Zepu Glaciers had a length up to ~80 km at the Baiyu Glacial Stage.

3 Methods

3.1 Theory of terrestrial cosmogenic radionuclide surface exposure dating

Terrestrial cosmogenic nuclides have been widely used in the studies of surface exposure ages and geomorphic evolution in recent years. In particular, surface exposure (SE) dating is applicable to Quaternary deglaciation events (e.g., glacial boulders and polished surfaces), and many significant associated results have been published^[6–9]. The theory of SE dating can be summarized as follows. Once the rocks buried deeply below the surface are exposed at the Earth's surface as a result of geological processes (e.g., Quaternary glaciation, landslide and debris-flow), the target elements (e.g., ¹⁶O, ²⁸Si, ⁴⁰Ca and ³⁵Cl) within the rocks are bombarded by secondary cosmic ray particles (e.g., fast neutrons, thermal neutrons and low negative muons), which causes nuclear reactions in forms of spallation, muon capture, etc., and formation of new, cosmogenic isotopes such as the radionuclides ¹⁰Be, ²⁶Al and ³⁶Cl, and stable ³He and ²¹Ne^[10]. The concentration of newly-formed isotopes is a function of exposure time of rocks and production rates of these nuclides. This can be expressed as

$$\frac{dN(x,t)}{dt} = -N(x,t)\lambda + P(x,t), \quad (1)$$

where N is the atomic number of a cosmogenic nuclide, x is the depth, t is the time, λ is the decay constant, and

P is the production rate, a function of depth and time. If samples are collected from a rock surface, the effect of depth on production rate can be ignored. Assuming constant production rate and zero erosion rate, eq. (1) can be simplified to

$$t = \frac{-1}{\lambda} \ln \left(1 - \frac{N\lambda}{P} \right). \quad (2)$$

3.2 Sampling

Samples for SE dating were collected by chiseling off ~2 kg of rock from the central part of the upper surfaces of quartz-rich boulders along moraine crests. Locations were chosen where there is no apparent evidence of slope instability. Accordingly, we chose boulders located at the relatively flat moraine crests and ones partly buried below the surface. The largest boulders (at least 1 m above the surface with the exception of Sample BYG-6) were chosen to help to reduce the effect of shielding by snow. Because erosion or weathering can reduce the nuclides near the surface, boulders with the least weathering (e.g., glacial striations and polished surfaces are present) were selected. The latitude, longitude and altitude of each sample location were measured using GPS and recorded. The width, length and height above the surface were also measured and recorded. Topographic shielding of cosmic rays by the surrounding mountains was determined by measuring the inclination from the boulder site to the top of the surrounding mountains. The inclination angle was measured every ten azimuth degrees, and all together 36 sets of data were obtained. In addition, the rock type and weathering characteristics of the samples were described. All these data were used to correct the cosmogenic ages of boulders. To make the ages systematically significant, 6–10 samples were collected from each moraine. However, due to the lack of funding, only three and nine samples on the moraines of Guxiang and Baiyu Glaciations, respectively, were measured and analyzed. The sample locations, altitudes and other associated parameters are shown in Figure 2 and Table 1.

3.3 Sample preparation

Sample preparation was completed at the Cosmogenic Nuclide Preparation Laboratory at University of Wisconsin-Madison and the preparation methods are from Bierman et al.^[11] A summary of the treatment procedures is as follows.

(1) Thicker samples were cut to less than 3 cm in

Table 1 Cosmogenic exposure ^{10}Be ages and associated parameters of the surface boulders of Guxiang and Baiyu Glaciations

Sample No.	Sample name	Latitude ($^{\circ}\text{N}$)	Longitude ($^{\circ}\text{E}$)	Elevation (m)	^{10}Be measured ($\times 10^6$ atom/g)	^{10}Be corrected ($\times 10^6$ atom/g)	^{10}Be exposure age (ka)
1	GX-1 a	29.912000	95.617500	2874	0.824 \pm 0.028	0.138 \pm 0.005	27.1 \pm 3.3
2	GX-1 b	29.912000	95.617500	2874	0.980 \pm 0.040	0.164 \pm 0.007	32.3 \pm 4.2
3	GX-3 a	29.912000	95.617500	2880	3.930 \pm 0.121	0.649 \pm 0.020	131.1 \pm 15.9
4	GX-3 b	29.912000	95.617500	2880	3.934 \pm 0.084	0.650 \pm 0.019	131.3 \pm 15.7
5	GX-4 a	29.906167	95.611667	2874	3.310 \pm 0.171	0.561 \pm 0.029	112.9 \pm 16.7
6	GX-4 b	29.906167	95.611667	2874	3.980 \pm 0.101	0.675 \pm 0.017	136.5 \pm 15.8
7	BYG-1	30.084500	95.531333	3009	0.458 \pm 0.014	0.071 \pm 0.002	13.9 \pm 1.6
8	BYG-3	30.097167	95.531167	3031	0.376 \pm 0.026	0.057 \pm 0.004	11.1 \pm 1.9
9	BYG-6	30.098167	95.523000	3049	0.190 \pm 0.009	0.028 \pm 0.001	5.6 \pm 0.8
10	BYG-9 a	30.099333	95.523000	3023	0.317 \pm 0.476	0.049 \pm 0.073	9.6 \pm 28.8
11	BYG-9 b	30.099333	95.523000	3023	0.614 \pm 0.020	0.094 \pm 0.003	18.5 \pm 2.2
12	BYG-11	30.101167	95.522333	3039	0.535 \pm 0.026	0.080 \pm 0.004	15.8 \pm 2.2
13	BYG-12	30.103333	95.522333	3022	0.508 \pm 0.021	0.078 \pm 0.003	15.3 \pm 2.0
14	BYG-13	30.098117	95.524333	3047	0.480 \pm 0.025	0.071 \pm 0.004	14.1 \pm 2.0
15	BYG-14	30.097667	95.524167	3049	0.397 \pm 0.021	0.059 \pm 0.003	11.7 \pm 1.7
16	BYG-19	30.105500	95.522500	3013	0.534 \pm 0.015	0.082 \pm 0.002	16.1 \pm 1.9

thickness. Then the samples were crushed using jaw crusher and disk grinder, and sieved using sieves. The 440–820 μm fraction of each sample was collected into labeled plastic bags. (2) Magnetic minerals were removed using a magnetic separator. (3) The samples were etched using HCl, HNO₃ and HF. HCl can effectively remove organic materials and most of the mafic minerals. Dilute HF/HNO₃ is used to dissolve mineral particles to make heavy liquid separation more effective. To improve efficiency, the etching should be done in an ultrasonic cleaner. (4) Density separation was undertaken to remove feldspars with density different from quartz. (5) 1% HF/HNO₃ was used to etch quartz to remove any remaining non-quartz minerals and meteoric ^{10}Be . Based on repeated experiments, it is more effective to carry out the first, second and third etchings in ultrasonic cleaner for 8, 14 and 24 h, respectively. (6) Inductively-coupled plasma atomic emission spectroscopy (ICP-AES) analysis was used to verify the quartz purity of the samples. If the quartz did not meet requirements, i.e. total Be at background levels (~ 0 μg) and total Al at or below 5 mg, Step (5) was repeated until satisfactory quartz purity was reached. (7) 500 μg of ^9Be carrier was added to 30–55 g quartz for each sample. ^{27}Al content of each sample was estimated based on the ICP-AES results. Additional ^{27}Al was added to some samples to ensure there was at least 4000 μg of total Al. The samples were then dissolved into HF/HNO₃. When dissolved completely, the samples were heated until they were dry. HCl was added to each sample. (8) For each batch of samples, two blanks were prepared to estimate the effect of environmental pollution (non-cosmogenic ^{10}Be and other elements) on the samples. 500 μg of ^9Be and 4000 μg of

^{27}Al were added to each blank. This was carried out simultaneously with Step (4) and the subsequent steps. (9) ICP-AES analysis was carried out for all samples and blanks. (10) Perchloric acid was added to all samples and blanks and heated to remove fluorine from BeF and AlF. (11) Anion exchange and precipitation were done to remove Fe and Ti from the samples. (12) Cation exchange was carried out to separate ^{10}Be from the samples. (13) Perchloric acid was added to the samples and blanks and heated to remove Bo. (14) NH₄OH was added to the samples. When the samples have PH values of 8–9, Be(OH)₂ will precipitate. In addition, Ca can be removed in this step. (15) The samples were heated at ~ 900 $^{\circ}\text{C}$ to oxidize Be(OH)₂ into BeO. (16) BeO was mixed with Ni being 3.5 times the sample mass. The samples were packed into targets and sent to the Purdue Rare Isotope Measurement Laboratory (PRIME Lab).

3.4 Sample measurement and analysis

The accelerator mass spectrum (AMS) measurement of ^{10}Be was completed at the PRIME Lab at Purdue University, USA. The measured isotope ratios of $^{10}\text{Be}/^9\text{Be}$ were converted to cosmogenic ^{10}Be concentrations in quartz using the total Be in the samples and the sample weights. The local production rates of ^{10}Be were calculated using a sea-level (1013.25 hPa) high latitude ($>60^{\circ}$) production rate of 5.1 atoms/g $\cdot\text{a}$ ^[12]. The relative contributions of spallogenic and muonic production are 97.4% and 2.6%, respectively^[12]. Atmospheric shielding of cosmic rays is determined in terms of atmospheric pressure rather than altitude. Ages were further corrected for changes in the paleo-geomagnetic field based on the data from Guyodo and Valet^[13] and McElhinny and

Senanayake^[14] using the methods suggested by Nishizumi^[15]. Corrections for the shielding of surrounding mountains and snow cover and corrections for sample thickness were made using the methods of Gosse and Philips. The results of measurement and analysis are shown in Table 1 and Figure 3.

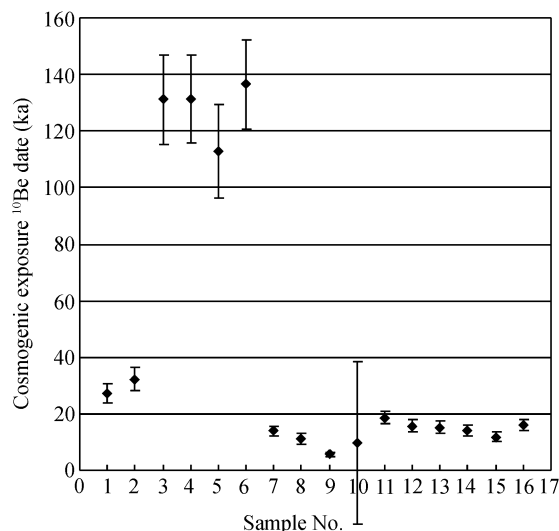


Figure 3 Distribution of the cosmogenic exposure dates and their errors of the surface boulders of the Guxiang and Baiyu Glaciations.

4 Discussion and conclusions

Each of the three samples (GX-1, 3 and 4) from the Guxiang Glaciation moraine and Sample BGY-9 from the Baiyu Glaciation moraine were divided into two portions. Consequently, two exposure ages were obtained for each of these samples. Samples GX-3 and GX-4, collected from the moraine crest, have ages varying from 112.9 ka BP to 136.5 ka BP. However, Sample GX-1 has ages of 27.1 ± 3.3 ka BP and 32.3 ± 4.2 ka BP, which can be assigned to MIS-2. As the boulder for Sample GX-1 is located near a gully, it cannot be precluded that the boulder rolled down from upper site and was exposed later. For the exposure ages of boulders from the Baiyu Glaciation moraines, with exceptions of BYG-9a and BYG-6, the other sample ages vary from 11.1 ka BP to 18.5 ka BP. Because the amount of Sample BYG-9a was not enough for AMS measurement, the age of 9.6 ± 28.8 ka BP has a large error and should be excluded from the age group. The boulder for Sample BYG-6 rises only 0.6 m above the surface, which is the minimum of all boulders. It is possible that the boulder was beneath the moraine surface when the glacier retreated, and that it cropped out only after several thou-

sand years of erosion. Consequently, the period of being exposed to cosmic rays is much shorter and the exposure age (5.6 ± 0.8 ka BP) of the boulder is much younger than the other boulders. In addition, thicker snow cover could occur on the boulder because of lower elevation above the surface, which could lead to a significant long-time of shielding of cosmic rays. This could be another reason of younger exposure age of the boulder.

Boulders begin to be bombarded by cosmic rays and new cosmogenic nuclides begin to form (the zero hour for cosmogenic exposure dating). To what extent do exposure ages of surface boulders on a moraine represent the timing of moraine formation or the beginning of deglaciation? This depends on how the moraine formed and how long it took. Some researchers have suggested that moraine construction is short-time process and that it only takes a few tens of years to several hundred years. In this case, the exposure ages of surface boulders can represent the timing of moraine deposition^[16–18]. By contrast, the construction of large moraines (e.g., moraines of Guxiang and Baiyu Glaciations in this study) on the Tibetan Plateau and Himalayas may need a long period of time. In this case, it is likely that the exposure ages of surface boulders are equivalent to the time of glacier retreat^[19]. In addition, erosion can affect the accumulation of cosmogenic nuclides to some extent. In particular, in areas like southeastern Tibet, the average annual precipitation is up to ~1000 mm at sampling altitudes. Obviously, this would lead to younger exposure ages. If considering all these factors, therefore, it can be concluded that the exposure ages (112.9–136.5 ka BP) of surface boulders on the Guxiang Glaciation moraine are likely to represent the timing of glacier retreat during the later part of the Guxiang Glaciation, and that exposure ages (11.1–18.5 ka BP) of the boulders on the Baiyu Glaciation moraine are equivalent to the timing of glacier retreat during the post-Last Glacial Maximum, and that the periods of the Guxiang and Baiyu Glaciations correspond to MIS-6 and MIS-2, respectively.

Much charcoal was collected from the bottom of colluvium overlying the Baiyu Glaciation moraine. The charcoal has ¹⁴C ages of 6290 ± 74 a BP and 6820 ± 280 a BP^[20]. The paleosol in the same layer as the charcoal was dated to ¹⁴C 6190 ± 75 a BP^[20]. The overlain paleosol has ¹⁴C ages of 3110 ± 85 a BP and 3420 ± 47 a BP^[20]. Considering that glacial retreat, soil development, forest formation, forest fire, together with colluvium deposition were a long-time process, the overlying charcoal

and paleosols with ^{14}C ages varying from 3110 ± 85 a BP to 6820 ± 280 a BP also provide an indirect evidence that the underlying Baiyu Glaciation moraine formed during MIS-2.

The glacial sediments themselves provide abundant information about glacial retreat during the later part of the Baiyu Glaciation. The glacier edge apparently stabilized at Linqiong for a long period of time and formed a set of extensive end moraine. Subsequently, the glacier tongue at Linqiong changed into stagnant ice, probably as a consequence of rapid rising of ELA. During this melting period, the stagnant ice formed the most extensive hummocky moraine on the Tibetan Plateau. This stagnation may be a typical response to abrupt climate change. The hummocky moraine was dated to ^{14}C 11252 ± 209 a BP^[21], and it is possible that this sudden climate change could be equivalent to the Bolling Warming event^[22]. Two sets of large moraines are present between the present end of the Zepu Glacier and

Yuren Village. The outer parts of these two sets of moraines are located at Baitong and Dana, 4 km and 7 km away from the contemporary glacier terminus, respectively. ^{14}C ages showed that the two sets of moraines formed during the Little Ice Age and Neoglaciation, respectively^[21].

The exposure dating of the glacial landforms of the Last Glacial Period in the Bodui Zangbo River valley has not been completed. In particular, the older samples collected from the moraine outside the MIS-2 moraine would provide more information about the timing of the Baiyu Glaciation. At present, it cannot be concluded that the older moraine formed during MIS-4 or MIS-3. Further work needs to be done.

The authors thank Brad Singer for guidance and R.A. Becker for his assistance in the lab. CRN analyses were provided by a Prime Lab Seed Grant to P. Colgan. Funding, lab equipment, and travel funds were provided by the Department of Geology at Grand Valley State University and the Department of Geology and Geophysics, University of Wisconsin—Madison.

- Li J J, Zheng B X, Yang X J, et al. Glaciers of Xizang (Tibetan) (in Chinese). Beijing: Science Press, 1986. 251—256
- Zhou S Z, Li J J, Li S J, et al. New understanding of Pleistocene glaciers in Qinghai-Tibetan Plateau. In: Quaternary Glacier & Environment Research Centre, ed. Quaternary Glacier and Environment Research in West China (in Chinese). Beijing: Science Press, 1991. 67—74
- Li J J, Zheng B X, Yang X J, et al. Glacier in Xizang (Tibetan) (in Chinese). Beijing: Science Press, 1986. 130—140
- Li B Y, Li J J. Quaternary Glacial Distribution Map of Qinghai - Tibetan Plateau (in Chinese). Beijing: Science Press, 1986
- Lanzhou Institute of Glaciology and Cryopedology, Academia Sinica. Glacier Inventory of China, Nyainqêntanglha Mountains (in Chinese). Beijing: Science Press, 1994
- Gosse J C, Klein J, Evenson E B, et al. Beryllium-10 dating of the duration and retreat of the last Pinedale glacial sequence. *Science*, 1995, 268 (5215): 1329—1333
- Phillips F M, Zreda M G, Benson L V, et al. Chronology for fluctuations in late Pleistocene Sierra Nevada glaciers and lakes. *Science*, 1996, 274 (5288): 749—751
- Gosse J C, Klein J, Evenson E B, et al. Precise cosmogenic ^{10}Be measurements in western North America: support for a global Younger Dryas cooling event. *Geology*, 1995, 23 (10): 877—880
- Brook E J, Brown E T, Kurz M D, et al. Constraints on age, erosion, and uplift of Neogene glacial deposits in the Transantarctic Mountains determined from in situ cosmogenic ^{10}Be and ^{26}Al . *Geology*, 1995, 23: 1063—1066
- Gosse J C, Phillips F M. Terrestrial in situ cosmogenic nuclides: theory and application. *Quat Sci Rev*, 2001, 20: 1475—1560
- Bierman P R, Caffee M W, Davis P T, et al. Rates and timing of earth surface processes from in-situ-produced cosmogenic Be-10. *Rev Miner*, 2002, 50: 147—196
- Stone J. Air pressure and cosmogenic isotopic production. *J Geophys Res*, 2000, 105 (B10): 23753—23759
- Guyodo Y, Valet J P. Relative variations in geomagnetic intensity from sedimentary records: the past 200 thousand years. *Earth Planet Sci Lett*, 1996, 143: 23—36
- McElhinny M W, Senanayake W E. Variations in the Geomagnetic Dipole I: The past 50000 years. *J Geomag Geoelectr*, 1982, 34: 39—51
- Nishizumi K, Winterer E L, Kohl C P, et al. Cosmic ray production rates of ^{10}Be and ^{26}Al in quartz from glacially polished rocks. *J Geophys Res*, 1989, 94: 17907—17915
- Gosse J C, Klein J, Evenson E B, et al. Beryllium-10 dating of the duration and retreat of the last Pinedale glacial sequence. *Science*, 1995, 268 (5215): 1329—1333
- Gosse J C, Klein J, Evenson E B, et al. Precise cosmogenic ^{10}Be measurements in western North America: support for a global Younger Dryas cooling event. *Geology*, 1995, 23 (10): 877—880
- Phillips F M, Zreda M G, Benson L V, et al. Chronology for fluctuations in late Pleistocene Sierra Nevada glaciers and lakes. *Science*, 1996, 274 (5288): 749—751
- Scott C H. Contemporary sediment transfer in Himalayan glacial systems, Unpublished PhD thesis, Leicester: University of Leicester, 1992. 352
- Zhou S Z, Li J J. A new study on Qinghai-Tibetan in ice age (in Chinese with English abstract). *Earth Sci Front* (in Chinese), 2001, 8 (1): 67—76
- Jiao K Q, Shuji I, Yao T D, et al. Variation of Zepu Glacier and environmental change in the eastern Nyainqêntanglha Range since 3.2 ka BP. *J Glaciol Geocryol* (in Chinese with English abstract), 2005, 27 (1): 74—79
- Yang W, Zhou S Z, Wang J, et al. Formation mechanism of hummocky moraine in the Bodui Zangbo Valley and its environmental significance. *J Glaciol Geocryol* (in Chinese with English abstract), 2005, 27 (2): 220—225